NUKLEONIKA 2004;49(3):115–121

Large Sample Neutron Activation Analysis: correction for neutron and gamma attenuation

Faidra Tzika,
Ion E. Stamatelatos,
John Kalef-Ezra,
Peter Bode

Abstract A Large Sample Neutron Activation Analysis (LSNAA) facility is under development at the GRR-1 research reactor, NCSR "Demokritos". The LSNAA facility design incorporates sample irradiation in the reactor graphite thermal neutron column and subsequent measurement of the activity induced in a gamma spectroscopy system with gamma ray transmission measurement options included. The Monte Carlo neutron and photon transport code MCNP-4C was used to model the facility. Appropriate correction factors accounting for neutron field perturbation during sample irradiation and high-purity germanium detector efficiency for the volume source were derived. The results of the computations were experimentally verified by measurements for a set of known materials. The LSNAA facility will be used to perform multi-element, non-destructive, contamination-free analysis of large volume samples with high sensitivity and excellent sampling. End-users of the facility will be archaeological, environmental, bio-medical research laboratories and industry.

Key words neutron activation analysis • neutron self-shielding • gamma ray attenuation • MCNP code

F. Tzika✉
Institute of Nuclear Technology and Radiation Protection,
NCSR "Demokritos",
15310 Aghia Paraskevi Attikis, Greece
and Medical Physics Laboratory,
Medical School,
University of Ioannina,
45110 Ioannina, Greece,
Tel.: +30 210 6503713, Fax: +30 210 6533431,
e-mail: faidra@ipta.demokritos.gr

I. E. Stamatelatos
Institute of Nuclear Technology and Radiation Protection,
NCSR "Demokritos",
15310 Aghia Paraskevi Attikis, Greece

J. Kalef-Ezra
Medical Physics Laboratory,
Medical School,
University of Ioannina,
45110 Ioannina, Greece

P. Bode
Interfaculty Research Institute,
Delft University of Technology,
15 Mekelweg, 2629 JB Delft, The Netherlands

Received: 2 February 2004, Accepted: 10 May 2004

Introduction

Most analytical techniques do not comply with the need for direct trace element analysis of samples exceeding the order of grams. Instead, sub-sampling methods are used to obtain representative sampling of the initial material. The possibilities arising from directly analyzing voluminous samples have been discussed [4]. Instrumental Neutron Activation Analysis (INAA) is a powerful technique, which can fulfil this need in a non-destructive way. For the quantitative analysis of large samples three parameters must be taken into consideration: neutron self-shielding during neutron irradiation, gamma ray attenuation within the sample during counting, and detector efficiency over the volume source.

At the GRR-1 research reactor, a LSNAA facility is under development for non-destructive determination of the elemental composition of large volume samples (i.e. volume up to ~5 liters). In the present work, the design of the facility is presented, as well as methods to correct the data for neutron and gamma ray self-shielding effects. The derivation of correction algorithms was based on modelling in detail, both the irradiation and counting facility using the Monte Carlo neutron photon transport code MCNP-4C [5]. Both the code and the cross-section data package were obtained from NEA Data Bank (France). The results of the computations were validated against experimental measurements.

Experimental setup

The technique consists of irradiation of the sample at the graphite thermal neutron column of the GRR-1 reactor and subsequent determination of the induced activity using HPGe spectroscopy. In case of an unknown material composition, a transmission measurement might be included for the determination of the effective linear attenuation coefficient of the sample.

Description of irradiation facility

GRR-1 is a 5 MW, open pool type, research reactor, cooled and moderated by light water, employing beryllium reflectors at two opposing sides of the core. A schematic representation of the core and graphite thermal column assembly is shown in Fig. 1. The thermal column (130 cm in height, 130 cm in width and 282 cm in length) is a stacking of graphite blocks. A 1 cm thick Boral^{TM} layer and a stainless steel layer of 1.2 cm shield the graphite stack. The rest of the shielding consists of barytes concrete. A 60 cm-long thermal column extension is placed between the core and the thermal column entrance surface. This consists of stacked graphite blocks within an aluminum container. Two additional lead blocks of 20 cm total thickness are placed between the core and the thermal column extension for gamma-ray shielding purposes.

The sample irradiation position was selected to be at 240 cm from the reactor core surface and at the mid-height of the fuel elements. At this location, the measured thermal neutron flux (sub-cadmium) was 4.5×10^6 cm^{-2}·s^{-1} and the thermal to non-thermal neutron flux ratio about 300. Thus, the effect of neutron moderation inside the sample may be considered negligible as only 0.3% of the neutrons entering the sample exceed the thermal energy region. Irradiation experiments were performed using the thermal column horizontal access through a concrete slide-door. However, the construction plans of the actual irradiation facility provide for a vertical access to the irradiation position thus enabling sample transferring during reactor operation time.

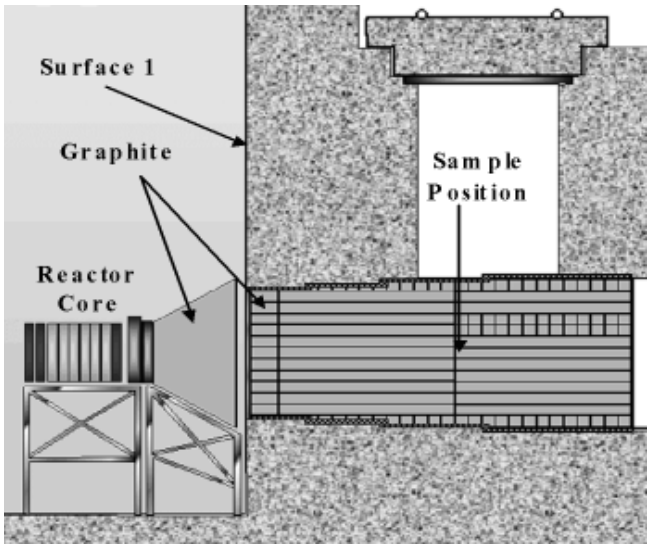

Fig. 1. Schematic representation of the GRR-1 core and graphite column (vertical cross-section).

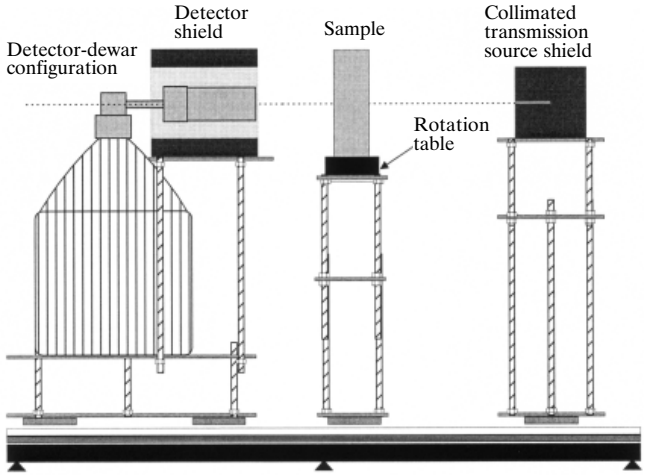

Fig. 2. Schematic representation of a spectroscopy and transmission measuring facility (vertical cross-section).

Description of counting facility

A counting facility was designed for LSNAA (Fig. 2). The system includes a holder for the detector and its shielding, sample positioning and transmission source support tables. All three parts are mounted on a base with adjusted aluminum linear guides, which provide a horizontal position adjustment of all three units.

The gamma ray spectrometer consists of an HPGe detector, GEM80 EG&G Ortec of 85% relative efficiency (nominal crystal dimensions of 81.5 mm in diameter and 57.7 mm in length), a digital signal processing data acquisition system, DSPEC-plus, PC-controlled by GammaVision software. The detector is housed in a lead shielding of 5 cm thickness. The sample is placed on a PC-controlled rotation table, supported by a base with vertical adjustment capability. The sample is positioned between the detector and the transmission source. A collimated ^{152}Eu source is used to assess the effective linear attenuation coefficient of samples made of unknown material, prior to the irradiation. The source is mounted in a lead shielding box offering a 5 mm diameter opening for source collimation.

Correction methods

Neutron self-shielding

A problem encountered during the irradiation of large samples is the perturbation of the neutron field due to absorption and scattering within the sample. Neutron flux is perturbed not only inside the sample, but may also be significantly perturbed in the graphite moderator in the vicinity of the sample. Therefore, both the self-shielding and flux depression factors have to be determined [9]. In the present study the self-shielding factor, f_n, is defined as the ratio of the average flux, $\bar{\Phi}_v$, throughout the volume of the sample to the average flux, $\bar{\Phi}_s$, at the entire surface of the sample. Flux depression factor, h_n, is defined as the ratio of the average flux, $\bar{\Phi}_s$, at the surface of the sample to the unperturbed flux, $\bar{\Phi}_r$, prior to the insertion of the sample. These factors depend on the neutron energy, the size and shape of the sample, as well as on the materials of the sample and surrounding medium.

A Monte Carlo model, including reactor core, thermal neutron column and sample, has been developed. The effects of chemical binding and crystal structure, for incident neutron energies below 4 eV at 300 K, were taken into account using the MCNP explicit S(a, b) capability. All runs were performed on a personal computer. Since geometry complexity is disadvantageous in terms of computation time, it was decided to use a simplified geometry model. Calculations performed for a detailed core geometry in criticality mode and a simplified homogenous core assembly with a Maxwell fission neutron source spectrum showed no difference in the thermal neutron flux distribution at the sample position. A significant gain in computation time was achieved by employing the Surface Source Write (SSW) option. Surface source was written at the front face of the graphite thermal column (surface 1, in Fig. 1) by recording the positions and the velocities of neutrons crossing the surface and entering the graphite column. The original number of histories used to write the SSW file, was 1×10^9 resulting in 1.6×10^6 tracks registered on the surface source. This file was then used as a source for subsequent MCNP simulations. Track length estimate tallies (F4) for neutron flux averaged over a cell in units of cm^{-2} per source neutron was used. The relative random errors of the computations were kept well below 10%. All statistical tests for the estimated answers were passed. The verification of the MCNP code predictions on the unperturbed thermal neutron flux at the thermal neutron column and its distributions in samples of known composition has been presented [16].

Neutron self-shielding and flux depression coefficients were determined for 130 homogeneous cylindrical samples made of various materials (among the 35 studied materials, ten contained significant amounts of hydrogen). The macroscopic thermal neutron absorption cross-sections of the materials ranged between 0.002 cm^{-1} and 24 cm^{-1}, and the scattering to total cross-section ratios between 0.01 and 0.98. Sample radius, r, ranged between 3 cm to 7.5 cm and height, h, between 10 cm to 30 cm.

Counting efficiency of the volume source

To obtain accurate results from gamma ray spectroscopy, a correction factor, that takes into consideration the source geometry as well as the gamma ray self-absorption and scattering by the sample material, has to be applied. The volume source efficiency correction factor, f_γ, is an energy, position and material dependent quantity. It is defined herein as the ratio of the volume source photopeak efficiency, ε_V, to the point source photopeak efficiency, ε_P, located at the centre of the sample, for a given photon energy, E_γ, and source to detector distance. Since it is impossible to obtain calibrated gamma ray voluminous sources for each sample under consideration, an MCNP model was developed to derive f_γ for energy and sample size ranges of interest.

A detailed detector geometry configuration was modelled using data provided by the manufacturer. Small discrepancies between the nominal and actual detector parameters may occur, in particular, with respect to the crystal active volume. To partially compensate for this effect, relative efficiencies were calculated. Pulse height tally, F8, was employed to determine the energy deposited in the crystal active volume in the specified energy bin. The relative random errors of the computations were kept below 2%. All statistical tests for the estimated answers were passed. The applicability of the detector model was validated against the measured relative off-axis efficiency values using a set of calibration point sources at distances up to ±12 cm both horizontal and vertical to the detector long axis.

The simulations were carried out assuming uniform radioactivity distribution over the entire volume (in daily practice the sample is going to be rotated along its vertical axis (Fig. 2) during counting). The "volume to point source" efficiency ratios were estimated for cylindrical samples representing a wide range of materials (Table 1). Their densities and mass attenuation coefficients are shown in Table 1 [8]. Calculations were performed for photon energies of 0.30, 0.66 and 1.33 MeV. The radius of simulated samples ranged between 4.3 cm and 7.5 cm and sample height between 9 cm to 30 cm.

Table 1. Materials simulated by MCNP and their mass attenuation coefficients.

Material	Density (g/cm^3)	μ/ρ ($\times 10^{-1}$ cm^2/g)		
		1332 keV	662 keV	303 keV
Paraffin	0.93	0.6312	0.8847	1.217
Water	1.00	0.6122	0.8572	1.182
Plexiglass	1.19	0.5940	0.8330	1.150
Cellulose	1.42	0.5847	0.8190	1.129
Calcium	1.55	0.5527	0.7789	1.111
SiO_2	2.32	0.5510	0.7729	1.072
Gypsum	2.32	0.5643	0.7919	1.105
Aluminum	2.70	0.5319	0.7468	1.038
Barium	3.50	0.4880	0.7766	1.861
Germanium	5.32	0.4938	0.7084	1.123
Chromium	7.18	0.5126	0.7249	1.061
Iron	7.92	0.5180	0.7366	1.093
Copper	8.94	0.5093	0.7262	1.112
Lead	11.35	0.5616	1.1010	3.949

Results and discussion

Neutron self-shielding

The self-shielding factor during neutron irradiation, f_n, depends on both the neutron diffusion length in the sample material, L, and the dimensions of the sample [10]. Therefore, in Fig. 3 the f_n data were plotted against the dimensionless quantity x_0, defined to be equal to $r \cdot h / [(r + h) \cdot L]$. The curve shown in Fig. 3 enables the determination of neutron self-shielding correction factors for large samples of known matrix. The self-shielding factor f_n is close to unity (>0.9) for $x_0 < 1$, drops to 0.5 at $x_0 = 3$, and below 0.15 at $x_0 > 15$. Therefore, the method is not proposed to be applied in samples with high x_0 values, due to errors related to the determination of f_n.

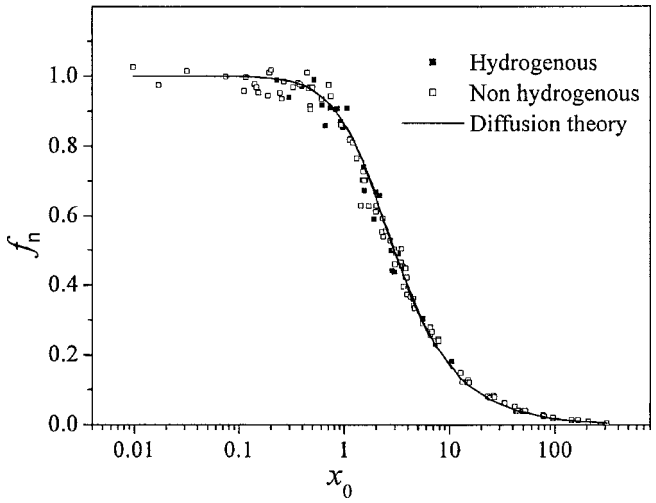

Fig. 3. Dependence of neutron self-shielding factor, f_n, on the dimensionless quantity $x_0 = r \cdot h/[(r + h) \cdot L]$.

In the daily practice of non-destructive LSNAA, the sample composition may not be known beforehand and, consequently, the curve presented in Fig. 3 cannot be directly used. Whenever this occurs, the neutron attenuating and scattering properties of the sample can be evaluated by measuring the thermal neutron flux at the sample surface [13].

The estimated flux depression factor, h_n, is shown in Fig. 4a as a function of the sample macroscopic thermal neutron absorption cross-section, Σ_a. Weak thermal neutron absorbers do not perturb the flux in the moderator ($h_n \approx 1$). However, in strongly absorbing materials significant flux depression occurs. The minimum h_n value is independent of the sample material and depends on the moderator material (graphite) and the sample dimensions.

The neutron self-shielding factor, f_n, is shown in Fig. 4b as a function of Σ_a. It is close to 1.0 for weakly neutron absorbing materials and tends to zero for strong absorbers. Therefore, whenever LSNAA is to be performed in samples of unknown composition, the measurement of the fluence rate at the sample surface and at a reference position away from the sample can be combined with the data shown in Fig. 4. The h_n and f_n values shown in Fig. 4 were obtained for cylindrical samples with $r \cdot h/(r + h)$ equal to 2.3, 4.0 and 7.5 cm. However, the calculations can be easily extended to include other sample sizes and shapes as well.

Counting efficiency of the volume source

A comparison between the MCNP calculated and experimentally measured off-axis relative efficiencies for the 1332 keV photopeak of a ^{60}Co point source, at 25 cm from the end-cap of the detector, is shown in Fig. 5a. The efficiency values are normalized to the 1332 keV efficiency on-axis at the same distance from the end-cap. The measured off-axis relative efficiencies, within a distance of ±12 cm from the detector axis, are predicted by the code with an accuracy of ±3%. The difference between predicted and experimentally determined relative efficiencies integrated over the range of y and z plotted areas is 0.8% and 1.3%, respectively.

In Fig. 5b, the ratio of the measured to calculated relative off-axis efficiencies for the 1332, 1173 and 662 keV photons is plotted against the horizontal distances, y, from detector axis, at the vertical plane 25 cm from the end-cap of the detector. Similar results were obtained for vertical distances, z, from detector axis. The measured off-axis relative efficiencies were in accordance within ±3%.

Whenever the sample to detector distance is much larger than the dimensions of the sample, interpolation of the transmission data obtained with the collimated ^{152}Eu source at the corresponding photon energy has to be carried out to estimate f_γ. However, whenever these sizes are comparable, an experimentally determined attenuation coefficient has to be coupled with the mean path length inside the sample of the emitted photons towards the effective volume of the detector. This quantity can also be determined by Monte Carlo simulation as proposed by Overwater *et al.* [12].

The efficiency correction factor of a uniform cylindrical source, f_γ, is shown in Fig. 6 as a function of the dimensionless variable, $\mu \cdot r \cdot h/(r + h)$, where μ is the linear attenuation coefficient (Table 1). Figure 6 reveals the universal applicability of the correction method for uniform samples

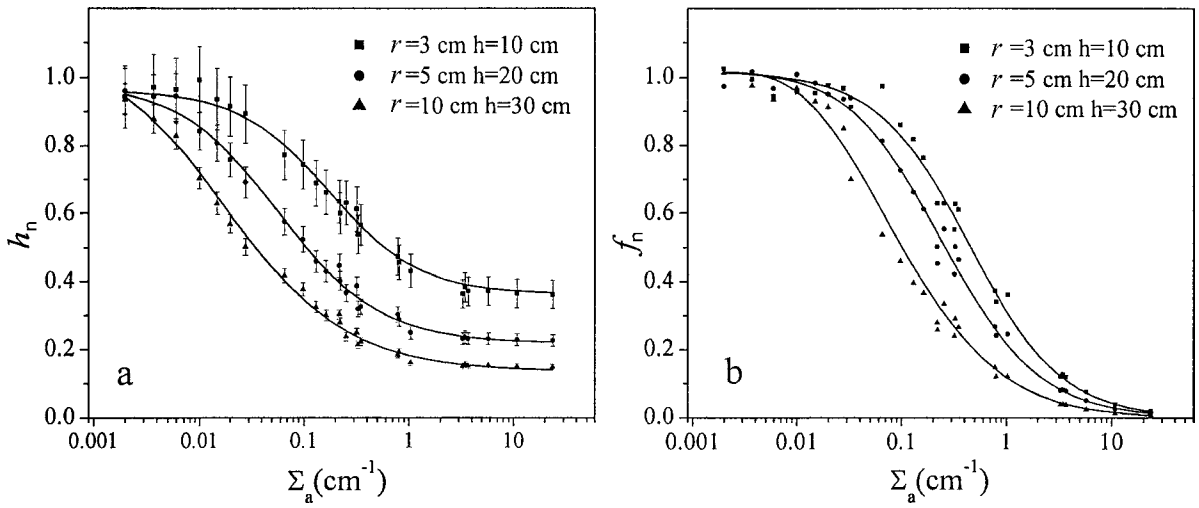

Fig. 4. a – Thermal neutron flux depression factor, h_n; b – thermal neutron flux correction factor, f_n, as a function of the macroscopic thermal neutron absorption cross-section, Σ_a, of cylindrical samples.

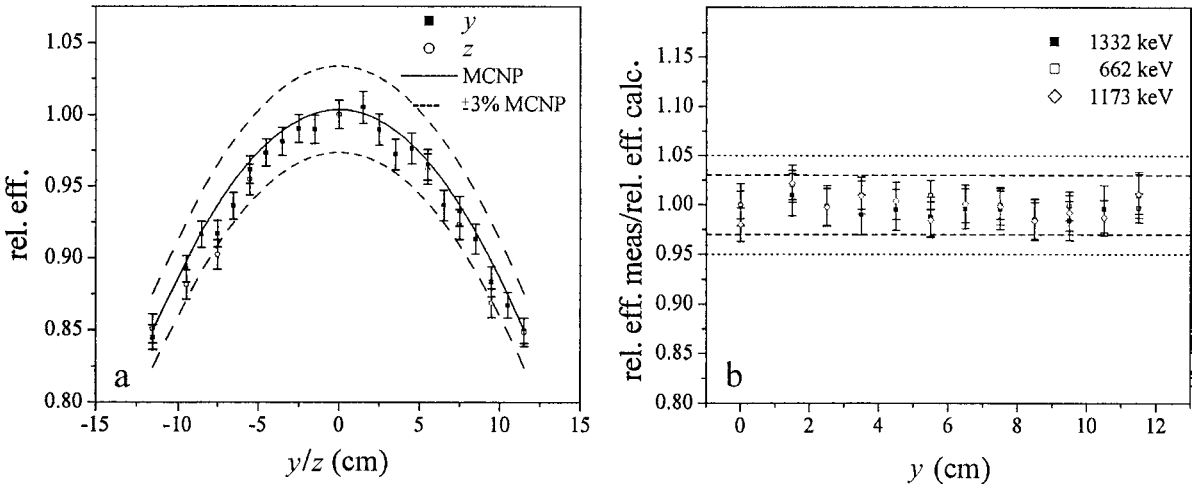

Fig. 5. a – Measured and calculated by MCNP off-axis to on-axis relative efficiencies for 1332 keV photons at a 25 cm distance from the end-cap of the detector; b – ratio of the measured to predicted relative off-axis efficiencies for 1332, 1173 and 662 keV photons as a function of distance from detector axis at a 25 cm distance from the end-cap.

of known composition. In case of samples of unknown composition, the linear attenuation coefficient assessed by a transmission measurement prior to the irradiation, has to be coupled with Fig. 6 to predict the f_γ value.

General discussion and conclusions

A Large Sample Neutron Activation Analysis facility is under development at GRR-1, NCSR "Demokritos". The facility design incorporates sample irradiation at the graphite thermal neutron column and subsequent measurement of the induced activity with a gamma spectroscopy system including options of gamma ray transmission measurement. The universal applicability of the technique requires correction algorithms for neutron self-shielding during sample irradiation, gamma ray attenuation within the sample during counting procedure and detector efficiency over the volume source.

Self-shielding correction methods for large sample irradiation have been proposed. Overwater *et al.* [13] developed a method based on neutron flux measurements at the vicinity of the sample and comparison with the neutron flux under reference conditions. Their neutron self-absorption method was based on a two-dimensional analytical solution of the diffusion equation for cylindrical samples [14]. The volume source efficiency was derived by integration of the detection probability (point source efficiency) and gamma ray attenuation fraction over the volume of the sample. The point source spatial efficiency function was determined by Monte Carlo calculations [12]. The method has been extended to allow the interpretation of scanned, collimated measurements, where results are obtained for individual voxels [2]. Shakir and Jervis [15] used neutron flux measurements to assess self-shielding factors for large cylindrical samples through adaptation of analytically derived values obtained from Fleming [7]. Degenaar and Blaauw [6], developed an empirical method to determine neutron self-shielding for large sample prompt-gamma neutron activation analysis by determination of macroscopic scattering and absorption cross-sections.

The derivation of correction algorithms, for the GRR-1 LSNAA facility, was based on a detailed model of both the irradiation and counting facilities using the Monte Carlo code MCNP-4C. The proposed neutron self-shielding correction method was in principle similar to the method developed at IRI, Delft [13]. Both methods depend on thermal neutron flux measurements at the vicinity of sample to derive appropriate neutron self-shielding correction factors. In this work, the Monte Carlo method was utilized to determine large sample neutron self-shielding factors. Advantages are better representation of the actual incident neutron field, sample geometry flexibility and the extension of the useful range of material applications to thermal neutron absorbing materials. The method is based on experimental determination of the flux depression factor and prediction of the self-shielding factor using the MCNP derived curves (Fig. 4).

A semi-empirical method to assess counting efficiency of photons for a cylindrical uniform volume source was considered. Correction factors, accounting for both the source geometry and the gamma ray attenuation in the sample, were derived via the experimentally validated detector model. A single semi-empirical curve was proposed (Fig. 6).

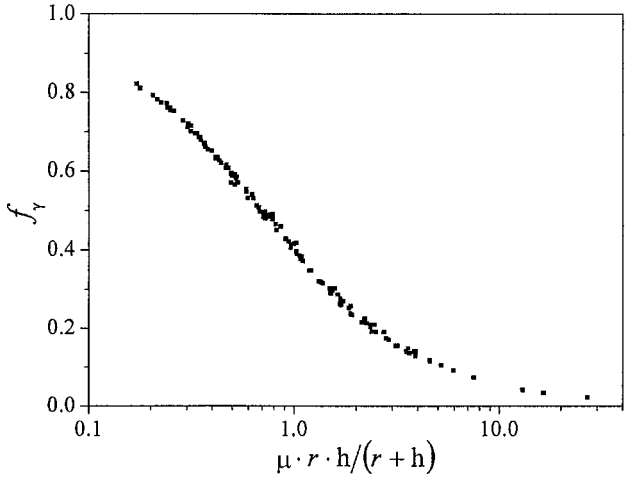

Fig. 6. Dependence of volume source efficiency correction factor, f_γ, on the sample dimensionless variable $\mu \cdot r \cdot h/(r + h)$.

The emerged calibration curve provides universal applicability, in terms of the range of photon energy, sample dimensions and material gamma attenuation properties of interest.

The method discussed is applicable to macroscopically homogeneous samples. However, sample inhomogeneity may significantly affect the accuracy of the results. Indications on sample matrix inhomogeneities can be obtained from the calculated values of linear attenuation coefficient for gamma radiation determined at various heights of the cylindrical sample. Moreover, inhomogeneities of the element to be determined can be revealed by conflicts in the analysis of the gamma ray spectrum when dealing with radionuclides emitting two or more gamma rays with different energies [3]. Studies performed by Overwater and Bode [11] have shown that, for samples of interest in large sample neutron activation analysis, the false concentrations may primarily be expected due to inhomogeneities of the element to be determined which affect the gamma ray attenuation. Nevertheless, Baas *et al.* [1] developed a gamma ray segment scanning technique in order to monitor large activated samples for the presence of extreme trace element inhomogeneities and determination of the spatial distribution of the induced activity.

In order to derive the magnitude of the effect of extreme trace element inhomogeneities, a set of MCNP runs was performed modelling "worst case" conditions in activity distribution within the activated sample. The simulations included: (a) activity distributed over the surface of the cylindrical sample; (b) linear activity distribution at the sample main axis; (c) activity at a point at the centre of the sample; (d) activity at a point at the centre of the top or bottom surface of the sample; (e) disk activity distribution over the top or bottom surface of the sample; (f) disk activity distribution at the centre of the sample. Calculations were performed for a series of samples of 1.6 L in volume (r = 5 cm and h = 20 cm), composed of water, graphite, iron and lead, emitting gamma rays of energies between 0.10 MeV and 1.5 MeV.

The ratio R, of the calculated correction factors for the inhomogeneous case, f_γ^i, to the correction factors for the case of homogeneous activity distribution in the same sample, f_γ^h, as a function of the linear attenuation coefficient, $\mu(E_\gamma)$, is shown in Fig. 7. The curves shown represent the upper limit of inaccuracy induced, with respect to the effect of inhomogeneities of trace element of interest, for samples of linear attenuation coefficient in the range between 0.05 cm^{-1} and 1 cm^{-1}. The most significant effects on R are observed when the trace element of interest is distributed either on the outside (point source at the top or bottom of the sample and surface source distribution) or on the main axis of the cylindrical sample. For the extreme element inhomogeneities examined the concentration can be determined within a factor of 1.25 and 4.5 for sample materials with linear attenuation coefficient of 0.1 cm^{-1} and 1 cm^{-1}, respectively. However, smaller values of R are expected in practice. Table 2 shows the derived values of R for example cases of materials and gamma ray energies of interest in large sample analysis. In particular, water and SiO_2 were considered to represent a biological and a geological material to be analyzed, respectively. From Table 2 it can be deduced that for water and SiO_2 the activity can be determined within a factor of 1.4 and 1.9, respectively.

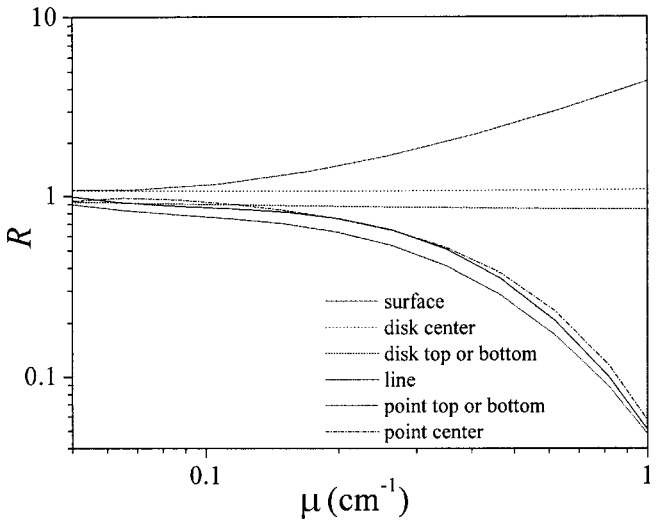

Fig. 7. The ratio R as a function of the linear attenuation coefficient, μ, for six cases of trace element inhomogeneities for a 1.6 L sample.

Table 2. Range of R values for water and SiO_2.

Material	Density (g/cm^3)	E_γ (keV)	μ (cm^{-1})	Range of R values
Water	1.00	300	0.119	0.74–1.21
		700	0.084	0.79–1.11
		1500	0.058	0.84–1.06
SiO_2	2.32	300	0.250	0.54–1.65
		700	0.175	0.66–1.39
		1500	0.120	0.73–1.21

The LSNAA facility at GRR-1 will be used to perform multi-element, non-destructive, contamination-free analysis of large volume samples with high sensitivity and excellent sampling. End-users of the facility are going to be biomedical, archaeological, environmental research laboratories as well as industry.

Acknowledgment This work was partially supported by the International Atomic Energy Agency, Vienna (Technical Cooperation program GRE/1/039). We acknowledge the assistance of GRR-1 technical staff during the experiments. We thank also Mr. N. Malliaros and Mr. G. Lefkopoulos for their technical contribution.

References

1. Baas HW, Blaauw M, Bode P, De Goeij JJM (1999) Collimated scanning towards 3D-INAA of inhomogeneous large samples. Fresenius J Anal Chem 363:753–759
2. Blaauw M, Baas HW, Donze M (2003) Height-resolved large-sample INAA of a 1 m long, 13 cm diameter ditch-bottom sample. Nucl Instrum Meth A 505:512–516
3. Bode P, Lakmaker O, Van Aller P, Blaauw M (1998) Feasibility studies of neutron activation analysis with kilogram-size samples. Fresenius J Anal Chem 360:10–17
4. Bode P, Overwater RMW (1993) Trace element determinations in very large samples: a new challenge for neutron activation analysis. J Radioanal Nucl Chem 167:169–176

5. Briesmeister JF (ed) (2000) MCNP – A General Monte Carlo N-Particle Transport Code, Version 4C. LA-13709-M. Los Alamos National Laboratory, Los Alamos, USA
6. Degenaar IH, Blaauw M, De Goeij JJM (2003) Correction for neutron self-shielding in large-sample prompt-gamma neutron activation analysis: determination of macroscopic neutron cross sections. J Radioanal Nucl Chem 257:467–470
7. Fleming RF (1982) Neutron self-shielding factors for simple geometries. Appl Radiat Isot 33:1263–1268
8. Hubbel JH, Seltzer SM (1995) Tables of X-ray mass attenuation coefficients and mass energy-absorption coefficients 1 keV to 20 MeV for elements $Z=1$ to 92 and 48 additional substances of dosimetric interest. NISTIR-5632
9. International Atomic Energy Agency (1970) Neutron fluence measurements. Technical Reports Series No 107. IAEA, Vienna
10. Meghreblian RV, Holmes DK (1960) Reactor analysis. McGraw-Hill Book Company Inc, New York
11. Overwater RMW, Bode P (1998) Computer simulations of the effects of inhomogeneities on the accuracy of large sample INAA. Appl Radiat Isot 8:967–976
12. Overwater RMW, Bode P, De Goeij JJM (1993) Gamma-ray spectroscopy of voluminous sources: corrections for source geometry and self-attenuation. Nucl Instrum Meth A 324:209–218
13. Overwater RMW, Bode P, De Goeij JJM, Hoogenboom JE (1996) Feasibility of elemental analysis of kilogram-size samples by instrumental neutron activation analysis. Anal Chem 68:341–348
14. Overwater RMW, Hoogenboom JE (1994) Accounting for the thermal neutron flux depression in voluminous samples for instrumental neutron activation analysis. Nucl Sci Eng 117:141–157
15. Shakir NS, Jervis RE (2001) Correction factors required for quantitative large volume INAA. J Radioanal Nucl Chem 248:61–68
16. Tzika F, Stamatelatos IE (2004) Thermal neutron self-shielding correction factors for large sample instrumental neutron activation analysis using the MCNP code. Nucl Instrum Meth B 213:177–181